Microbial Factor-Mediated Development in a Host-Bacterial Mutualism

Tanya A. Koropatnick,[1] Jacquelyn T. Engle,[2] Michael A. Apicella,[3] Eric V. Stabb,[4] William E. Goldman,[2] Margaret J. McFall-Ngai[1,5]*

Tracheal cytotoxin (TCT), a fragment of the bacterial surface molecule peptidoglycan (PGN), is the factor responsible for the extensive tissue damage characteristic of whooping cough and gonorrhea infections. Here, we report that *Vibrio fischeri* also releases TCT, which acts in synergy with lipopolysaccharide (LPS) to trigger tissue development in its mutualistic symbiosis with the squid *Euprymna scolopes*. As components of PGN and LPS have commonly been linked with pathogenesis in animals, these findings demonstrate that host interpretation of these bacterial signal molecules is context dependent. Therefore, such differences in interpretation can lead to either inflammation and disease or to the establishment of a mutually beneficial animal-microbe association.

To date, molecules conserved among microbes, such as LPS and PGN, have been collectively described as "pathogen"-associated molecular patterns (PAMPs) (*1*). However, the majority of animal-microbe interactions are benign or mutualistic, raising the question: What role might such factors play in other types of host-microbe associations?

The reciprocal dialogue between partners in benign host-symbiont associations has been shown to be important for host tissue maturation (*2*–*4*), although the identification of the bacterial signals involved has proven elusive. The symbiosis between the Hawaiian bobtail squid *E. scolopes* and the luminous, Gram-negative bacterium *V. fischeri* offers the opportunity to decipher experimentally the precise dialogue between host and microbe partners. In this system, the bacterium colonizes epithelium-lined crypts within the host's light-emitting organ as a monospecific, extracellular symbiont (Fig. 1) (*5*).

Shortly after the juvenile squid emerges from the egg, the bacterial inoculum is gathered from the environment as seawater passes through the mantle cavity (*6*). Two prominent fields of ciliated epithelia on the surface of the squid's light organ facilitate the colonization process through ciliary motion and mucus shedding, resulting in the aggregation of symbiont cells above pores on the surface of the organ. Once aggregated, the symbionts migrate through the pores, down ducts, and into crypts that are located 100 to 200 μm from the surface epithelia (Fig. 1). Upon colonization of the crypts, some of the first processes triggered by the symbiont include the infiltration of macrophage-like hemocytes (blood cells) into the sinuses of the ciliated fields (Fig. 2A) and the induction of widespread apoptosis of the epithelial cells that compose these fields (*5*) (Fig. 2B). The most conspicuous response to light organ colonization is the extensive morphogenesis of the organ's surface, which culminates in the complete loss of the ciliated field 4 days after the initial colonization by the symbiont (Fig. 2C). In nature, only *V. fischeri* is capable of colonizing the crypts and signaling this morphogenesis, which serves to transform the organ from a morphology associated with the colonization process to one characteristic of the mature, functional organ. PGN in ambient seawater is known to trigger the shedding of mucus from the epithelial fields of the light organ (*7*), and LPS can induce low levels of early-stage apoptosis (*8*). However, the symbiont-derived factor(s) capable of triggering the full sequence of light organ morphogenesis have yet to be identified.

V. fischeri continuously sheds fragments of its surface in culture, and the crypt epithelial cells that interface closely with the symbiont cross-react with a monoclonal antibody to *V. fischeri* LPS (*9*). Cell surface fractions isolated from *V. fischeri* were sufficient to induce levels of hemocyte infiltration, apoptosis, and regression of the epithelial fields comparable to those induced by the intact symbiont (Fig. 2, D to F). Cell surface fractions from the nonsymbiotic, marine, Gram-negative bacterium *Pseudoalteromonas luteoviolacea* were also active (*9*).

V. fischeri PGN signaled levels of hemocyte infiltration comparable to those initiated by the intact symbiont, whereas *V. fischeri* LPS did not induce this cellular reaction (Fig. 2G). Alone, PGN did not trigger apoptosis, although LPS did stimulate it at low levels; however, together PGN and LPS acted synergistically to induce apoptosis at levels characteristic of those resulting from colonization by the intact symbiont (Fig. 2H). PGN, both alone and in synergy with LPS, also induced significant levels of epithelial regression (Fig. 2I). These findings are similar to those reported for certain pathogenic associations in which PGN and PGN fragments can induce macrophage activation (*10*) and infiltration (*11*) into inflamed host tissues. Likewise, purified PGN and LPS work in synergy to

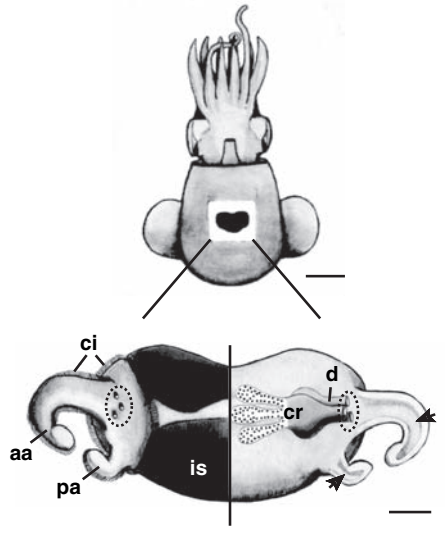

Fig. 1. *E. scolopes* possesses a light-emitting organ. (**Top**) A ventral view of a juvenile squid shows a window through the mantle to illustrate the position of the organ within the mantle cavity. Scale bar, 500 μm. (**Bottom**) An enlargement shows the details of the juvenile light organ morphology. The left half illustrates the surface with its ciliated epithelial field, which is composed of an anterior (aa) and posterior (pa) appendage and a base with three pores (circled) that lead to internal epithelium-lined crypts. The right half is a frontal section through the organ showing these epithelium-lined crypts (cr) containing the bacteria (stippled) within crypt diverticula and the relation of the crypts and ducts to the pores (circled), which open onto the surface. This section also shows the sinuses (arrows) within the appendages. The sinus spaces are continuous with the circulatory system and separate from the bacteria-containing crypts. ci, cilia; d, ducts; is, ink sac. Scale bar, 150 μm.

[1]Pacific Biomedical Research Center, Kewalo Marine Laboratory, University of Hawaii, 41 Ahui Street, Honolulu, HI 96813, USA. [2]Department of Molecular Microbiology, Washington University School of Medicine, St. Louis, MO 63110, USA. [3]Department of Microbiology, University of Iowa, Iowa City, IA 52242, USA. [4]Department of Microbiology, University of Georgia, Athens, GA 30602, USA. [5]Department of Medical Microbiology and Immunology, University of Wisconsin, 1300 University Avenue, Madison, WI 53706, USA.

*To whom correspondence should be addressed. E-mail: mjmcfallngai@wisc.edu

trigger inflammatory cytokine release, nitric oxide production, and organ injury in a rat model of bacterial sepsis (*12*).

Because mixed fragments of PGN with LPS could not consistently induce regression to the extent elicited by the intact symbiont (Fig. 2I), we reasoned that *V. fischeri* might have an active mechanism to release specific PGN fragments to the host, as opposed to the passive release due to cell lysis. Specific release of peptidoglycan by growing cells has only been observed in cultures of *Bordetella pertussis* (*13*) and *Neisseria gonorrhoeae* (*14*), both of which release large amounts of peptidoglycan monomers. The best studied of these fractions is tracheal cytotoxin (TCT; *N*-acetylglucosaminyl-1,6-anhydro-*N*-acetylmuramylalanyl-γ-glutamyldiaminopimelylalanine) (Fig. 3A), a disaccharide-tetrapeptide monomer of PGN, which causes the epithelial cytopathology of pertussis (*15*) and gonococcal infections (*16*). Fractionation of culture supernatants of *V. fischeri* by reversed-phase HPLC revealed a peak with an elution time identical to that of TCT. When purified, this fraction contained three amino acids: alanine, glutamic acid, and diaminopimelic acid,

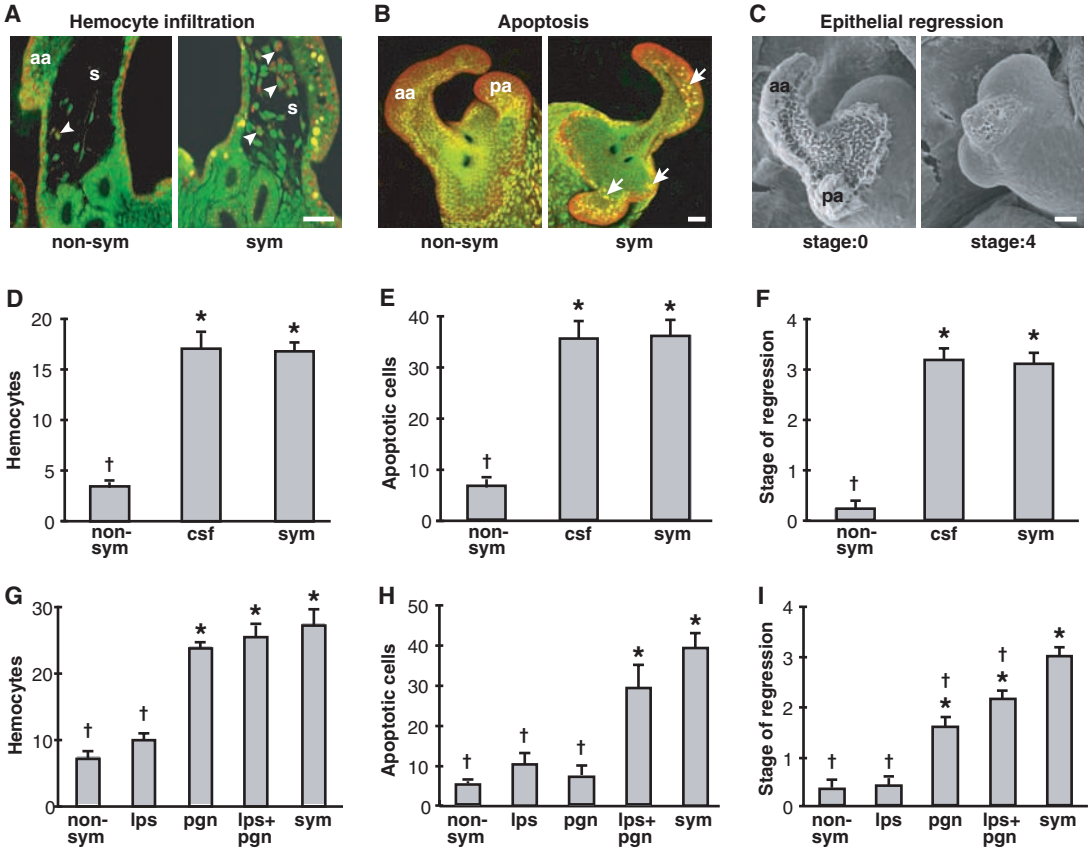

Fig. 2. Bacterial components induce light organ morphogenesis. (**A** and **B**) Confocal micrographs of nonsymbiotic [non-sym, i.e., uninfected (*25*)] and symbiotic (sym) organ epithelial fields stained with acridine orange (green) and Lysotracker (red). (A) Hemocytes (arrowheads) within the appendage sinuses (s). (B) Apoptotic cells, yellow foci (arrows). (**C**) SEMs of epithelial fields before (stage 0) and after (stage 4) regression. Scale bar, 50 μm. (**D** to **F**) Effects of *V. fischeri* cell surface fractions (csf) on hemocytes infiltration (D), induction of apoptosis (E), and epithelial regression (F). Animals were exposed to surface fractions at a protein concentration of 100 μg/ml of seawater. (**G** to **I**) Effects of *V. fischeri* surface components, LPS (10 μg/ml) and PGN (50 μg/ml), on hemocyte infiltration (G), induction of apoptosis (H), and epithelial regression (I). Data are means ± SEM for one of three replicate experiments (n = 8 to 12 per treatment). (*) indicates significant (P < 0.001) difference compared with non-sym. (†) indicates significant (P < 0.001) difference compared with sym.

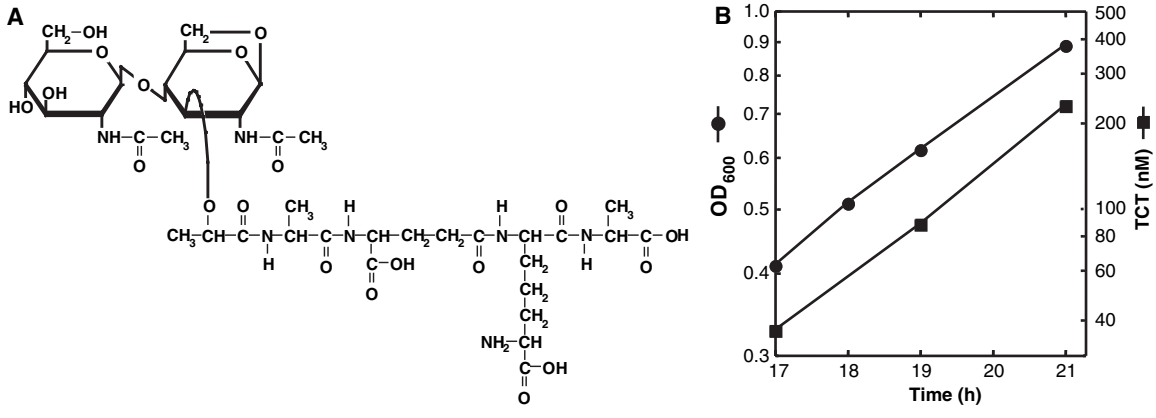

Fig. 3. TCT, a monomer of PGN, is released by growing cells of *V. fischeri*. (**A**) Structure of TCT. *V. fischeri* strain ES114 was cultured at room temperature in defined medium HM (*26*) supplemented with 2% glucose. A released fragment of *V. fischeri* PGN was determined to be identical to TCT by subjecting culture supernatants to solid phase extraction and two reverse-phase HPLC steps, as described for *B. pertussis* (*13*). A peak with an elution time corresponding to *B. pertussis* TCT was collected and further characterized by amino acid analysis and by matrix-assisted laser desorption mass spectrometry (*25*). (**B**) Production of TCT during a 4 hour period of log-phase growth. For sensitive quantification of TCT production, broth cultures were inoculated at OD_{600} = 0.04, after which log-phase *V. fischeri* culture supernatants were collected, subjected to solid phase extraction (*13*), and derivatized with phenylisothiocyanate. The resulting phenylthiocarbamyl (PTC) derivatives were separated by reversed-phase high-performance liquid chromatography using a C_8 column and detected at 254 nm. The amount of *V. fischeri* PTC-TCT in each sample was determined by comparing the peak area and elution time with an identically processed TCT standard. Results are representative of two experiments.

in molar proportions of 2:1:1. Mass spectrometry revealed a single species with a mass of 921 daltons. These data correspond precisely to TCT (*17*). Unlike most Gram-negative bacteria, *V. fischeri*, like *B. pertussis* (*18*), actively released appreciable amounts of TCT during log-phase growth (Fig. 3B).

TCT alone triggered hemocyte infiltration and regression of the epithelial fields at levels similar to those induced by intact *V. fischeri* (Fig. 4, A and C). TCT induced epithelial regression 4 days after exposures as brief as 14 hours (*9*), a time course similar to the intact symbiosis (*19*). The concentration of TCT required to trigger a detectable morphogenic response was as little as 10 nM, and the response was saturated at concentrations as low as 1 μM (0.9 μg/ml) (*9*). Comparatively, PGN, a multimer of TCT subunits, was generally not active below 50 μg/ml, and constant exposure was necessary to trigger epithelial regression by 4 days. To determine how specific the morphogenic responses were to TCT, we also tested muramyl dipeptide and glucosylmuramyl dipeptide, which are two smaller components of PGN known to signal host cell responses in various mammalian model systems (*20*, *21*). No morphogenic activity was detected in squid light organs when exposed to these components, either alone or in combination with LPS (*9*).

Under the conditions of the assay, TCT also triggered levels of apoptosis in the epithelial fields similar to those observed in the intact symbiosis (Fig. 4B), whereas LPS-free PGN did not induce apoptosis (Fig. 2H). Thus, the background level of LPS in the natural seawater, which typically ranges from 0.01 to 1.5 ng/ml (*22*), was sufficient to act together with the more potent TCT to induce the apoptotic effect (Fig. 4B). However, as cells of *V. fischeri* naturally colonize the crypts in high numbers and subsequently trigger morphogenesis from within these spaces (*19*), it is likely to be symbiont-specific LPS which works in concert with TCT to induce morphogenesis.

These results show that growing cells of *V. fischeri* release TCT, which acts as a potent morphogen to induce normal light organ morphogenesis in the squid host. Similar morphogenic effects of TCT have been reported for both *B. pertussis* and *N. gonorrhoeae*, which induce the loss of ciliated cells from mammalian respiratory and fallopian tube epithelia, respectively (*15*, *16*). In addition, TCT works in synergy with LPS to stimulate the production of inflammatory cytokines, nitric oxide, and the inhibition of DNA synthesis in hamster tracheal epithelium (*23*). In these studies, TCT-induced epithelial morphogenesis resulted from a direct interaction with the target epithelium. Note that, in the squid light organ, morphogenesis is triggered from within the crypt spaces, several cell layers away from the target epithelium (*19*). Thus, it will be interesting to identify and localize the TCT receptor(s) within the light organ and to decipher the host pathways that mediate these remote events.

These findings, as well as recent studies of mechanisms of tolerance to gut microbiota (*24*), demonstrate that "PAMPs" may be too narrow an acronym for eukaryotic-prokaryotic signaling associated with microbial molecules, such as LPS and PGN. The data suggest that a more general term, such as microbe associated molecular patterns (MAMPs), would be more appropriate to describe factors conserved and essential to the biology of microbes, which mediate recognition and response during host-microbe interactions.

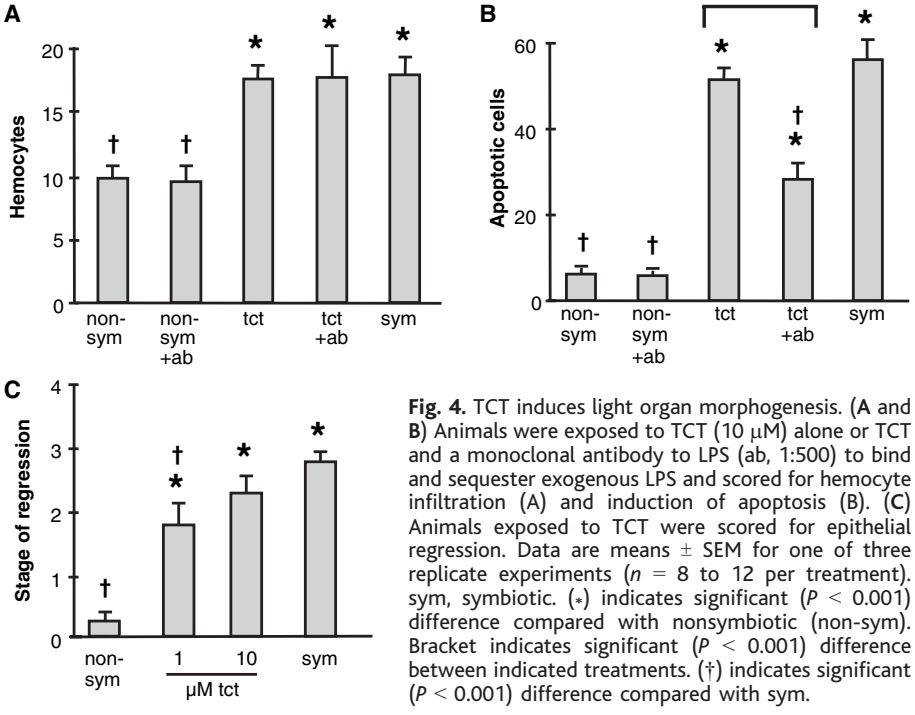

Fig. 4. TCT induces light organ morphogenesis. (**A** and **B**) Animals were exposed to TCT (10 μM) alone or TCT and a monoclonal antibody to LPS (ab, 1:500) to bind and sequester exogenous LPS and scored for hemocyte infiltration (A) and induction of apoptosis (B). (**C**) Animals exposed to TCT were scored for epithelial regression. Data are means ± SEM for one of three replicate experiments (n = 8 to 12 per treatment). sym, symbiotic. (*) indicates significant ($P < 0.001$) difference compared with nonsymbiotic (non-sym). Bracket indicates significant ($P < 0.001$) difference between indicated treatments. (†) indicates significant ($P < 0.001$) difference compared with sym.

References and Notes

1. R. Medzhitov, C. A. Janeway Jr., *Science* **296**, 298 (2002).
2. L. V. Hooper, *Trends Microbiol.* **12**, 129 (2004).
3. J. Xu, J. I. Gordon, *Proc. Natl. Acad. Sci. U.S.A.* **100**, 10452 (2003).
4. M. J. McFall-Ngai, *Dev. Biol.* **242**, 1 (2002).
5. S. V. Nyholm, M. J. McFall-Ngai, *Nature Rev. Microbiol.*, **2**, 632 (2004).
6. S. V. Nyholm, E. V. Stabb, E. G. Ruby, M. J. McFall-Ngai, *Proc. Natl. Acad. Sci. U.S.A.* **97**, 10231 (2000).
7. S. V. Nyholm, B. Deplancke, H. R. Gaskins, M. A. Apicella, M. J. McFall-Ngai, *Appl. Environ. Microbiol.* **68**, 5113 (2002).
8. J. S. Foster, M. A. Apicella, M. J. McFall-Ngai, *Dev. Biol.* **226**, 242 (2000).
9. M. J. McFall-Ngai *et al.*, unpublished observations.
10. M. J. Pabst, S. Beranova-Giorgianni, J. M. Krueger, *Neuroimmunomodulation* **6**, 261 (1999).
11. Z. Q. Liu, G. M. Deng, S. Foster, A. Tarkowski, *Arthritis Res.* **3**, 375 (2001).
12. G. M. Wray, S. J. Foster, C. J. Hinds, C. Thiemermann, *Shock* **15**, 135 (2001).
13. B. T. Cookson, H. L. Cho, L. A. Herwaldt, W. E. Goldman, *Infect. Immun.* **57**, 2223 (1989).
14. R. S. Rosenthal, *Infect. Immun.* **24**, 869 (1979).
15. W. E. Goldman, D. G. Klapper, J. B. Baseman, *Infect. Immun.* **36**, 782 (1982).
16. M. A. Melly, Z. A. McGee, R. S. Rosenthal, *J. Infect. Dis.* **149**, 378 (1984).
17. B. T. Cookson, A. N. Tyler, W. E. Goldman, *Biochemistry* **28**, 1744 (1989).
18. R. S. Rosenthal, W. Nogami, B. T. Cookson, W. E. Goldman, W. J. Folkening, *Infect. Immun.* **55**, 2117 (1987).
19. J. A. Doino, M. J. McFall-Ngai, *Biol. Bull.* **189**, 347 (1995).
20. N. Inohara *et al.*, *J. Biol. Chem.* **278**, 5509 (2003).
21. S. Traub *et al.*, *J. Biol. Chem.* **279**, 8694 (2004).
22. D. M. Karl, F. C. Dobbs, in *Molecular Approaches to the Study of the Ocean*, K. E. Cooksey, Ed. (Chapman and Hall, London, 1998), pp. 29–89.
23. T. A. Flak, L. N. Heiss, J. T. Engle, W. E. Goldman, *Infect. Immun.* **68**, 1235 (2000).
24. S. Rakoff-Nahoum, J. Paglino, F. Eslami-Varzaneh, S. Edberg, R. Medzhitov, *Cell* **118**, 229 (2004).
25. Materials and methods are available on *Science* Online.
26. E. G. Ruby, K. H. Nealson, *Appl. Environ. Microbiol.* **34**, 164 (1977).

27. We are grateful to C. Chun, W. Crookes, M. Goodson, J. Graber, D. Millikan, E. Ruby, and A. Schaefer for critical reading of this manuscript; M. McMahon for technical assistance; and C. Yap for Fig. 1 illustrations. We also thank M. Hadfield for the provision of *P. luteoviolacea*. Supported by an NIH grant to M.M.-N., M.A.A., and E.V.S. (grant no. R01-AI50661), an NSF grant to M.M.-N. (grant no. IBN0211673), an NIH grant to E. G. Ruby and M.M.-N. (grant no. NCRR12294), a W. M. Keck Foundation grant to M.M.-N. and M.A.A., and a Canadian NSERC scholarship to T.A.K.

Supporting Online Material

www.sciencemag.org/cgi/content/full/306/5699/1186/DC1
Materials and Methods
References

1 July 2004; accepted 21 September 2004